Supporting Information

Rashkovan et al. 10.1073/pnas.1412107111

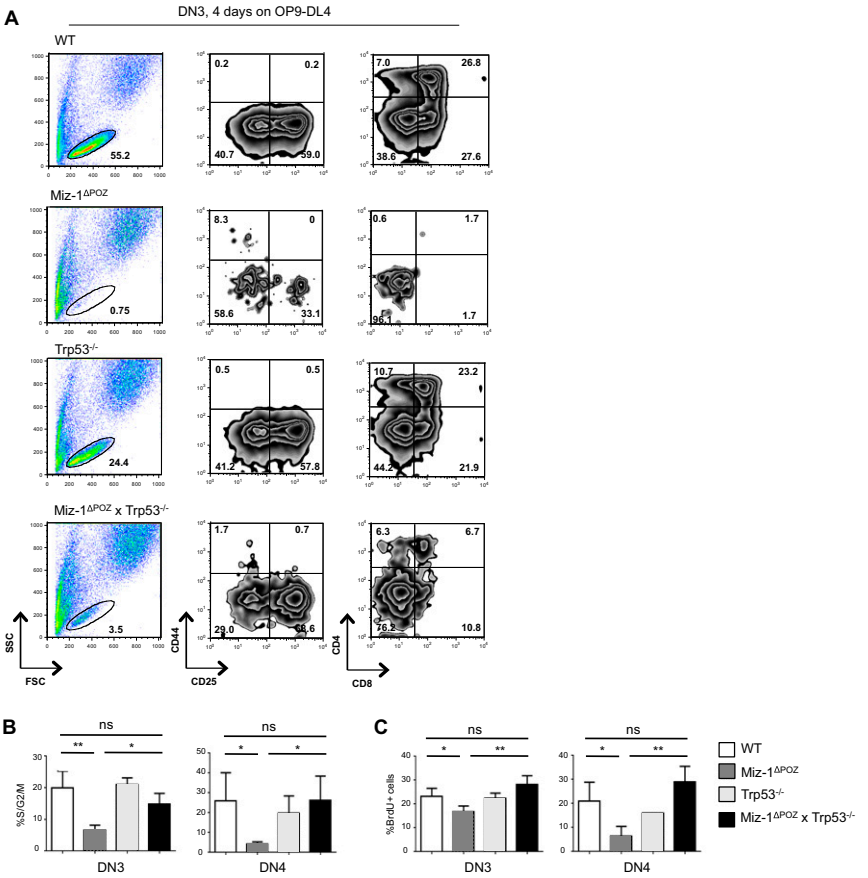

Fig. S1. Deletion of p53 restores the ability of Miz-1$^{\Delta POZ}$ pre-T cells to differentiate in vitro. (*A*) DN3 pre-T cells from WT, Miz-1$^{\Delta POZ}$, *Trp53*$^{-/-}$, and Miz-1$^{\Delta POZ}$ × *Trp53*$^{-/-}$ mice were sorted onto OP9-DL4 and analyzed for CD25, CD44, CD4, and CD8 surface expression after 4 d in culture. Data are representative of three independent experiments. (*B*) Cell cycle analysis using PI staining performed on sorted, permeabilized DN3 and DN4 cells. Graph shows percentages of cells in S/G2/M phases of the cell cycle. Data are averaged from three independent experiments and are presented as mean ± SD. (*C*) Cell cycle analysis after in vivo BrdU labeling. Graph shows percentages of BrdU^{+} DN3 and DN4 cells. Data are averaged from three independent experiments and are presented as mean ± SD.

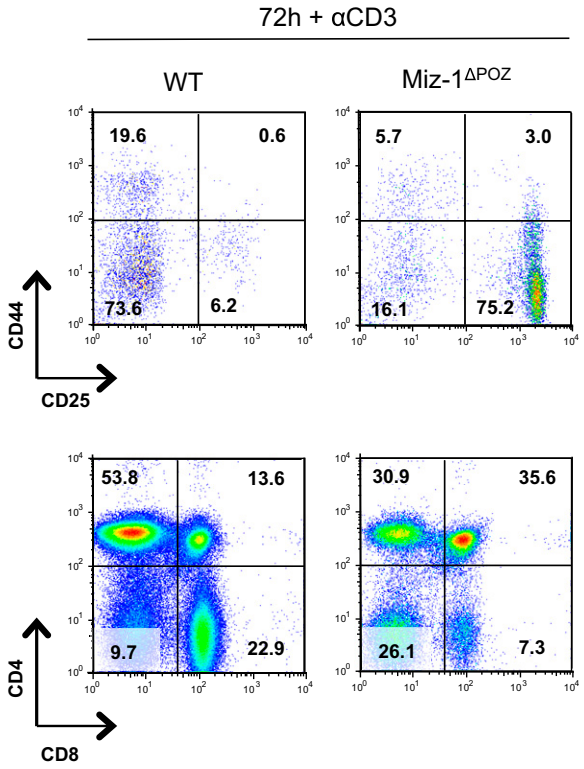

Fig. S2. Mitogenic stimulation of WT and Miz-1$^{\Delta POZ}$ pre-T cells. FACS analysis of WT and Miz-1$^{\Delta POZ}$ pre-T cells at 72 h after injection with αCD3.

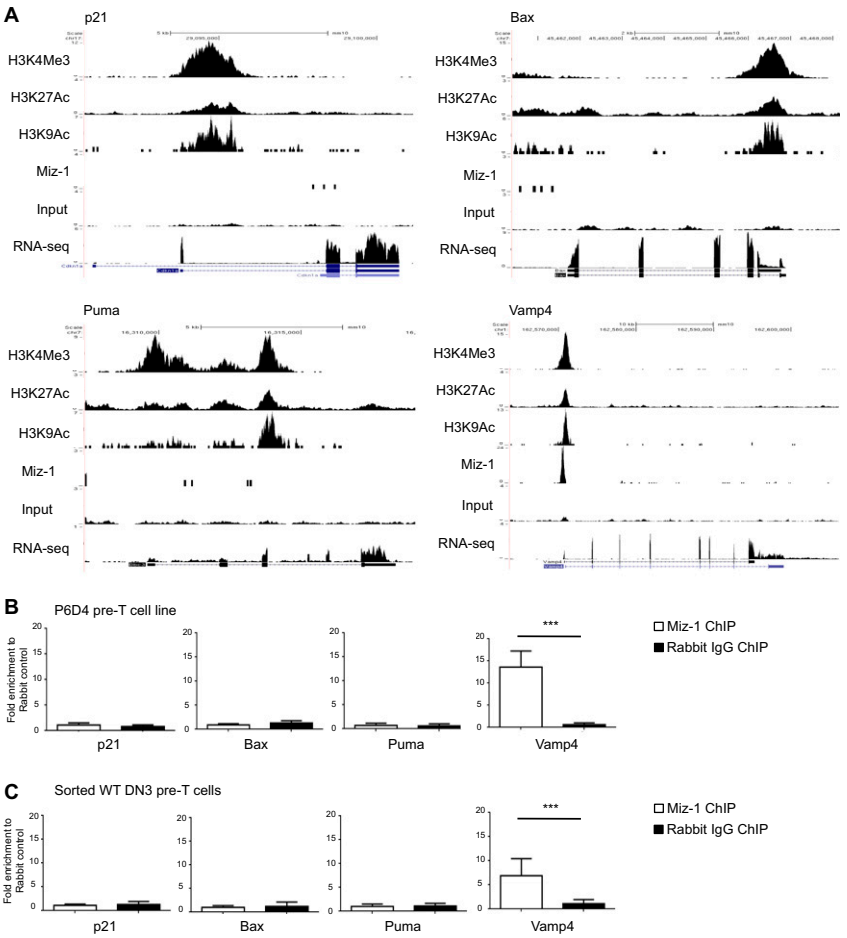

Fig. S3. Miz-1 does not directly regulate the expression of p53 target genes in DN3 pre-T cells. (*A*) ChIP-seq experiments for Miz-1 and histone activation marks (H3K4Me3, H3K27Ac, and H3K9Ac) in P6D4 murine pre-T cells. Shown are p53 target genes (*p21*, *Bax*, and *Puma*) and a positive control for Miz-1 binding and activation (*Vamp4*). Scale is in number of reads per million reads. (*B*) ChIP-qPCR experiments to determine possible binding of Miz-1 to the promoters of p53 target genes in murine P6D4 pre-T cells. Graph shows fold enrichment of anti-Miz-1 ChIP over rabbit IgG control ChIP. The *Vamp4* promoter contains a Miz-1–binding site and is used as a positive control for the Miz-1 ChIP. Data are represented as average fold change ± SD from at least three independent experiments. (*C*) ChIP-qPCR experiments to determine possible binding of Miz-1 to the promoters of p53 target genes in sorted primary DN3 cells. Graph shows fold enrichment of anti–Miz-1 ChIP over rabbit IgG control ChIP. Data represent as average fold change ± SD from at least three independent experiments.

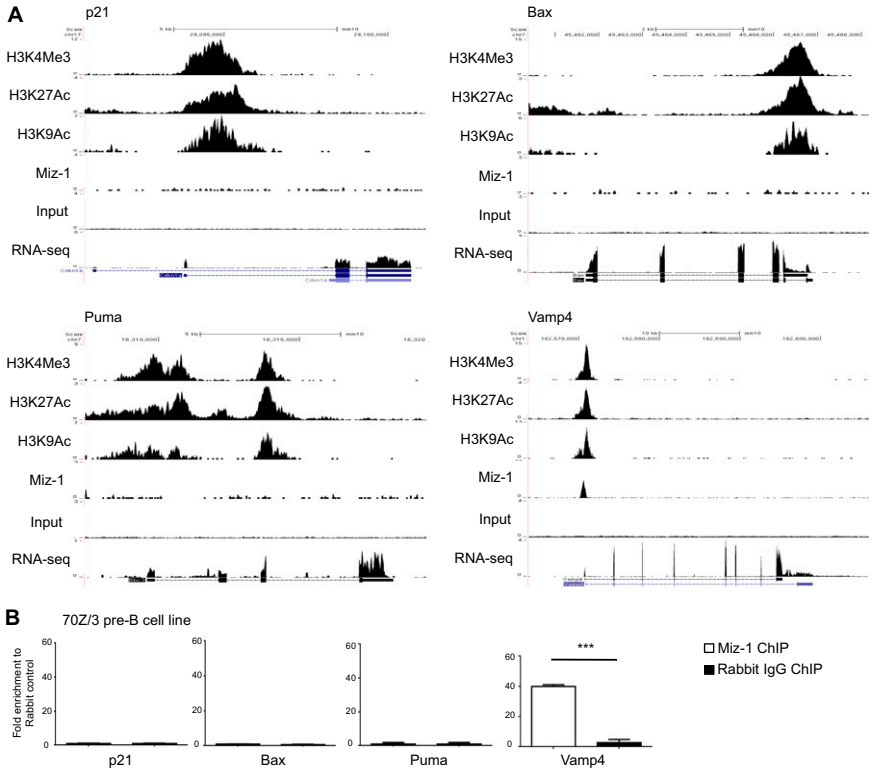

Fig. S4. Miz-1 does not directly regulate the expression of p53 target genes in pre-B cells. (*A*) ChIP-seq experiments for Miz-1 and histone activation marks (H3K4Me3, H3K27Ac, and H3K9Ac) in a 70Z/3 pre-B cell line. Shown are p53 target genes (*p21*, *Bax*, and *Puma*) and a positive control for Miz-1 binding and activation (*Vamp4*). Scale is in number of RPM. (*B*) ChIP-qPCR experiments to determine possible binding of Miz-1 to the promoters of p53 target genes in 70Z/3 pre-B cells. Graph shows fold enrichment of anti–Miz-1 ChIP over rabbit IgG control ChIP. The *Vamp4* promoter contains a Miz-1–binding site and serves as a positive control for the Miz-1 ChIP. Data represent average fold change ± SD from at least three independent experiments.

Table S1. qPCR primer sequences

Primer	Sequence	Reference
Cdkn1a (p21) forward	AGATCCACAGCGATATCCAGAC	(1)
Cdkn1a (p21) reverse	ACCGAAGAGACAACGGCACACT	
Puma (Bbc3) forward	ACGACCTCAACGCGCAGTACG	(1)
Puma (Bbc3) reverse	GAGGAGTCCCATGAAGAGATTG	
Bax forward	CAGGATGCGTCCACCAAGAA	(1)
Bax reverse	AGTCCGTGTCCACGTCAGCA	
Gapdh forward	TTCCGTGTTCCTACCCCCAATG	(2)
Gapdh reverse	GGAGTTGCTGTTGAAGTCGCAG	
P53 forward	AAGACAGGCAGACTTTTCGCC	(3)
P53 reverse	CGGGTGGCTCATAAGGTACC	
Actin forward	CTCTGGCTCCTAGCACCATGAAGA	(4)
Actin reverse	GTAAAACGCAGCTCAGTAACAGTCCG	
Rpl22 forward	AGGTGCCTTTCTCCAAAAGGTATT	This study
Rpl22 reverse	AAACCACCGGTTTTGTTCCT	
Rpl22l1 forward	TGGAGGTTTCATTTGGACCTTAC	(5)
Rpl22l1 reverse	TTTCCAGTTTTTCCATTGACTTTAAC	

1. Li T, et al. (2012) Tumor suppression in the absence of p53-mediated cell-cycle arrest, apoptosis, and senescence. *Cell* 149(6):1269–1283.
2. Kosan C, et al. (2010) Transcription factor miz-1 is required to regulate interleukin-7 receptor signaling at early commitment stages of B cell differentiation. *Immunity* 33(6):917–928.
3. Hattangadi SM, Burke KA, Lodish HF (2010) Homeodomain-interacting protein kinase 2 plays an important role in normal terminal erythroid differentiation. *Blood* 115(23):4853–4861.
4. Stephens AS, Stephens SR, Morrison NA (2011) Internal control genes for quantitative RT-PCR expression analysis in mouse osteoblasts, osteoclasts and macrophages. *BMC Res Notes* 4:410.
5. O'Leary MN, et al. (2013) The ribosomal protein Rpl22 controls ribosome composition by directly repressing expression of its own paralog, Rpl22l1. *PLoS Genet* 9(8):e1003708.

Table S2. ChIP-qPCR primer sequences

Primer	Sequence	Reference
Cdkn1a (p21) forward	CGCTGCGTGACAAGAGAATA	(1)
Cdkn1a (p21) reverse	CCTCCCCTCTGGGAATCTAA	
Puma (Bbc3) forward	CTTGTGCCCCAGCTTTCAT	(1)
Puma (Bbc3) reverse	GAGTCCCAGGTGCTTCCTTC	
Bax forward	CGGCAATTCTGCTTTAACCT	(1)
Bax reverse	CGCCCCCATTATTTCTTCTT	
Gapdh forward	Gtgttcctacccccaatgtg	This study
Gapdh reverse	ggagacaacctggtcctcag	
Vamp4 forward	AGTCACCCTTTCAGCTCCAG	This study
Vamp4 reverse	TCAGATCCGATGGAGGAGCA	
Rpl22_2 forward	Tccctgagtcattcgcagt	This study
Rpl22_2 reverse	cttttcccagggcgaagt	
Rpl22_3 forward	Cagttcctaactggcgttgg	This study
Rpl22_3 reverse	agcctcagcccagagaatg	

1. Khandanpour C, et al. (2013) Growth factor independence 1 antagonizes a p53-induced DNA damage response pathway in lymphoblastic leukemia. *Cancer Cell* 23(2):200–214.